

# OPTIMIZATION AND DESIGN GUIDELINES FOR HIGH FLUX MICRO-CHANNEL HEAT SINKS FOR LIQUID AND GASEOUS SINGLE-PHASE FLOW

Norbert Müller, Luc G. Fréchette  
Mechanical Engineering  
Columbia University in the City of New York  
P.O. Box 12345  
New York, NY, USA, 10027  
Phone: (212) 854-2962  
Fax/Voice: (347) 412-7848  
Email: norbertmueller@yahoo.com  
Web: www.columbia.edu/~lf307

## ABSTRACT

A numerical optimization tool is used to optimize forced convection micro-channel heat sinks for minimum pump power at high heat fluxes. Results gained with the optimization tool are generalized and optimum configurations are illustrated on design charts. Physical trends are illustrated analytically using the underlying relations.

Investigations are done for air and water in single-phase flow with no phase transition; with hydraulic diameters of the micro-channels ranging from about 1 micron to 80 mm. Optimization is shown to have a tremendous effect. It can reduce pump power by several orders of magnitude, especially for high heat flux devices. Using water and air as coolants, designs for heat fluxes of  $>10 \text{ kW/cm}^2$  and  $>100 \text{ W/cm}^2$  respectively with pump/fan power expenses less than 1% are easily found with the optimization tool. It appears that large aspect ratios for the flow channels are favorable for high heat fluxes in micro heat sinks. For each design, there exists an optimum fin height and ratio of fin thickness to channel width. The design space investigation also suggests that short channels in multiple parallel units are a key feature of compact high heat flux heat sinks. Practical design examples underline the feasibility of the results and general design guidelines are derived.

**KEY WORDS:** MEMS, IC cooling, finned surface, maximum heat transfer, minimum pump power

## NOMENCLATURE

A	area, $\text{m}^2$
c	velocity, $\text{m/s}$
cF	velocity factor, (-)
$c_p$	specific heat coefficient, $\text{J/kg/K}$
C	fin constant, $1/\text{m}$
$D_h$	hydraulic diameter, $\text{m}$
H	fin height (channel height), $\text{m}$
h	heat transfer coefficient, $\text{W/m}^2/\text{K}$
F	function
f	friction factor, (-)
k	thermal conductivity, $\text{W/m/K}$
L	length, $\text{m}$
m	mass flow rate, $\text{kg/s}$
N	number of channels per fin unit, (-)
Nu	Nusselt number, (-)

P	fan/pump power, $\text{W}$
p	pressure, $\text{Pa}$
q	heat flux, $\text{W/m}^2$
Q	heat rate, $\text{W}$
Re	Reynolds number, (-)
S	shape factor, (-)
T	temperature, $\text{K}$
U	number of fin units, (-)
W	channel width, $\text{m}$

## Greek symbols

$\alpha$	fin unit angle, $^\circ$
$\Delta$	difference
$\vartheta$	temperature difference, $\text{K}$
$\delta$	thickness, $\text{m}$
$\eta$	fan/pump efficiency, (-)
$\eta_f$	fin efficiency, (-)
$\eta_o$	overall surface efficiency, (-)
$\nu$	kinematic viscosity, $\text{m}^2/\text{s}$
$\rho$	density, $\text{kg/m}^3$
$\zeta$	loss coefficient, (-)

## Subscripts

1	inlet
2	outlet
add	additional
b	base
corr	corrected
Cu	copper
f	fin
m	logarithmic mean, mean
max	maximum
Opt	optimum
Si	silicon
U	fin unit

## INTRODUCTION

The rapid increase in power densities of ICs has induced a permanent interest in new reliable and high heat flux cooling technologies [1, 2]. In parallel, there has been an interest in optimizing conventional heat sinks, in which a single-phase fluid is forced over a finned surface [3, 4]. These heat sinks are mostly chosen for their low manufacturing costs. So today, extruded heat sinks with ducted fans are the standard for processors in many computer systems. In addition, ongoing

research in the area of micro thermo-fluid systems raises the need for high flux heat exchangers using a liquid or gaseous working fluid, for devices such as micro chemical reactors, refrigeration cycles on-a-chip, microfabricated heat engines, and portable fuel cells. A comprehensive analysis of studies on heat transfer and fluid flow in micro-channels over the past decade can be found in Sobhan and Garimella [5].

For forced convection, the heat flux increases with smaller flow channels and - when the channels are rectangular - with higher aspect ratio. But also, the necessary fan/pump power for forcing the coolant through the channels increases at smaller scales.

In this work, a simple optimization tool is described and used to optimize fin geometry and coolant volume flow. For a given base and required heat removal, the optimization consists of finding the optimum geometric configuration of the fins that requires the least pump power to force the coolant through.

Unlike Copeland [4], Tuckerman and Pease [3], the current analysis assumes no limits or set values for fin thickness, channel width and height as well as pump power or flow velocity. The objective is to find the optimum design for each condition in a large design space independent of the chosen manufacturing approach. However, if necessary such limits easily can be implemented.

### Configurations

Figure 1a shows a regular finned base, where the parallel fins have the same length as the base and the coolant flows from one end to the other along a single channel formed between the fins.

Instead of extending the fins over the entire length of the base, they can be divided in  $U$  units, each a fraction of the base length. Fresh coolant is introduced at the beginning and heated coolant discharged at the end of each unit (Figure 1b). As will be shown, the through flow velocity and in turn pressure loss and pump power can be reduced for similar or higher heat flux. However, to realize this approach a longer base is necessary to account for the space required for the inlet and discharge of coolant to each unit ( $(U-1)L_{\text{add}}$ ) as illustrated in Figure 1c.

This additional spacing can be alleviated, by arranging the fin units side-by-side, as shown in Figure 1d. This configuration requires a heat spreader if the heat is not generated in long narrow bands, which could be imagined for future fuel cell ribbons and some electronic or electric devices.

When the pressure loss of the coolant inlet and outlet between the fin units in Figure 1c is taken into account, it appears that a zigzag arrangement of the fin units like in Figure 1e can reduce the overall pressure loss.

### Approach

In either configuration, the analysis is centered on determining the heat removal rate and fluid power requirements. The approach consists of analytically modeling the heat transfer and pressure drop and defining the geometry and flow that result in minimal pump/fan power for a specified heat removal requirement and base area. In the following sections, the governing equations for a set number of fin units (as in Figures 1a, b and d) are outlined and algebraically combined

to analytically determine the impact of as many design parameters as possible. A numerical optimization is then used for the remaining parameters and the results are presented on design charts. The analysis is then extended to include inlet and exit losses for the zigzag configuration, where the unit layout introduces additional independent variables, which are numerically optimized, beside the height and aspect ratio of the fins and channels.

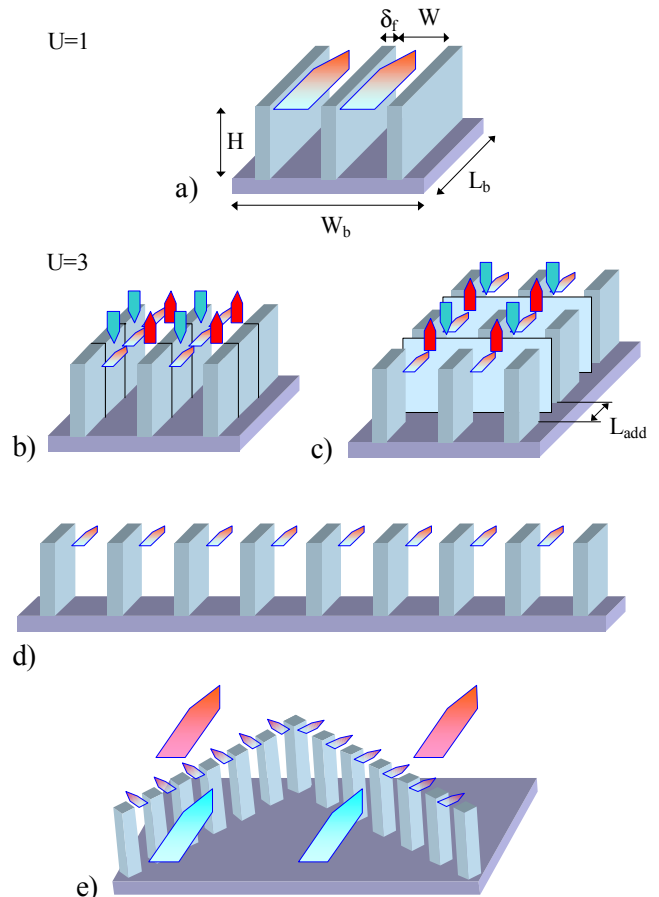


Fig. 1: Heat Sink configurations: a) regular finned base, b) fins divided in fin units with fresh coolant introduced into each unit, c) a longer base accounts for the space required for coolant inlet/outlet of each unit, d) side-by-side arrangement of fin units alleviates additional spacing for inlet/outlet, e) zigzag arrangements of the fin units can reduce overall pressure loss compared to c)

### ANALYSIS

Each design point is specified by the following parameters: the heat rate to be removed  $Q$ , the available heat sink base area  $A_b$ , base aspect ratio  $W_b/L_b$  and the chosen number of units  $U$ , which can be combined into a shape factor (Equation 18), the base temperature  $T_b$ , the thermal conductivity of the heat sink material  $k_f$ , and the chosen cooling fluid and its approach temperature  $T_1$  (Table 1a). The following analysis is reduced to the base surface and the fins themselves. It does not include the thickness of the base (substrate).

## Hydrodynamic analysis

The fan/pump power  $P$  is calculated for incompressible flow,

$$P = \frac{\Delta p \cdot m}{\eta \cdot \rho} \quad (1)$$

where the quotient of the mass flow rate  $m$  and density  $\rho$  is the volume flow rate and  $\eta$  is a overall efficiency of the fan/pump.  $\Delta p$  is the pressure drop across the heat sink,

$$\Delta p = f \cdot \frac{L_U}{D_h} \cdot \frac{\rho}{2} \cdot c^2 = \zeta \cdot \frac{\rho}{2} \cdot c^2 \quad (2)$$

$\rho$  is the density of the fluid,  $L_U$  is the length of a fin unit (fin length) and  $\zeta = f L_U / D_h$  is the loss coefficient. The hydraulic diameter  $D_h$  is defined as:

$$D_h = \frac{2 \cdot H \cdot W}{H + W} \quad (3)$$

with  $H$  being the fin height and  $W$  the channel width (distance between two neighboring fins). Assuming fully developed laminar flow, the friction factor  $f$  is calculated by interpolation of tabulated numerical solutions  $fRe = \{56.92; 62.2; 68.36; 72.92; 78.8; 82.32; 96\}$  for aspect ratios  $H/W = \{1; 2; 3; 4; 6; 8; \infty\}$ ,  $f = fRe(H/W) / Re$  [6],

$$Re = \frac{D_h \cdot c}{\nu} \quad (4)$$

The kinematic viscosity  $\nu$  is assumed as the mean of the inlet and outlet values. The through flow velocity  $c$  is the mean velocity in the flow channels, defined as:

$$c = \frac{m}{\rho \cdot H \cdot W \cdot N \cdot U} \quad (5)$$

where  $\rho$  is a mean value for the fluid density,  $N = W_U / (W + \delta_f)$  is the number of channels per fin unit and  $U$  the number of fin units.

## Convection analysis

The necessary mass flow rate  $m$  is calculated from the heat rate to be removed  $Q$ ,

$$m = \frac{Q}{c_p \cdot (\vartheta_1 - \vartheta_2)} \quad (6)$$

using the specific heat coefficient  $c_p$  of the fluid and the temperature differences of the base against the fluid  $\vartheta = T_b - T$  at the fin unit inlet and outlet, assuming uniform base temperature  $T_b$ .

The outlet temperature difference is determined by the logarithmic mean temperature difference,

$$\vartheta_m = \frac{\vartheta_2 - \vartheta_1}{\ln(\vartheta_2 / \vartheta_1)} \quad (7)$$

that is necessary to remove the desired heat rate  $Q$

$$\vartheta_m = \frac{Q}{A_U \cdot h \cdot \eta_o \cdot U} \quad (8)$$

from a certain fin geometry, where  $A_U$  is the total heat transfer surface of a fin unit

$$A_U = N \cdot L_U \cdot (2H + \delta_f + W) \quad (9)$$

and  $\delta_f$  is the fin thickness. The heat transfer coefficient  $h$  is,

$$h = \frac{k \cdot Nu}{D_h} \quad (10)$$

where  $k$  is the thermal conductivity of the fluid. Assuming fully developed laminar flow, the Nusselt number is calculated by interpolation of tabulated numerical solutions for uniform wall temperature  $Nu = \{2.98; 3.08; 3.39; 3.96; 4.44; 5.6; 7.54\}$  and aspect ratios  $H/W = \{1; 2; 3; 4; 6; 8; \infty\}$  [6].

The overall surface efficiency of one fin unit  $\eta_o$  in Equation 8 is calculated by

$$\eta_o = 1 - \frac{A_f}{A_U} \cdot (1 - \eta_f) \quad (11)$$

with the fin area of one fin unit  $A_f$

$$A_f = N \cdot L_U \cdot (2H + \delta_f) \quad (12)$$

and the fin efficiency  $\eta_f$  [7],

$$\eta_f = \frac{\tanh(C \cdot H_{corr})}{C \cdot H_{corr}} \quad (13)$$

where  $H_{corr} = H + \delta_f / 2$  is a corrected fin height for an active fin tip [8].

$$C = \sqrt{\frac{2h}{k_f \cdot \delta_f}} \quad (14)$$

The fin constant  $C$  contains an approximated fin perimeter  $2L_U$  [9].

## Combined analysis

For analysis purposes, it is convenient to combine the above equations to the extent possible. Since Equations 7 and 13 cannot be solved algebraically for the desired variables, the above equations are combined into three subsets.

Introducing the dimensionless parameters  $H/W$ ,  $\delta_f/W$  and  $W_b/L_b$  Equations 1-6 can reduce to:

$$P \cdot \eta = \frac{Q^2}{(\vartheta_1 - \vartheta_2)} \cdot \frac{\nu}{\rho \cdot c_p} \cdot Geo1 \quad (15a)$$

with:

$$Geo1 = fRe(H/W) \cdot \frac{(1 + H/W)^2 \cdot (1 + \delta_f/W)}{8 \cdot W_b/L_b \cdot U^2 \cdot H^2} \quad (15b)$$

Figure 2 shows the relationship  $\vartheta_2 = F(\vartheta_m)$  which is implicit in Equation 7.

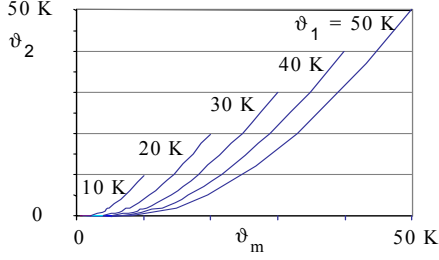


Fig. 2: Logarithmic mean temperature (Equation 7)

Equations 8-12 can combine to:

$$\vartheta_m = \frac{Q}{k \cdot A_b \cdot \text{Geo2}} \quad (16a)$$

with:

$$\text{Geo2} = \text{Nu}(H/W) \cdot \frac{(1+H/W) \cdot [1 + (2 \cdot H/W + \delta_f/W) \cdot \eta_f]}{2 \cdot H \cdot (1 + \delta_f/W)} \quad (16b)$$

Introducing the same dimensionless parameters  $H/W$  and  $\delta_f/W$  in Equation 13, gives:

$$\eta_f = \frac{\tanh(\text{Geo3} \cdot \sqrt{k/k_f})}{\text{Geo3} \cdot \sqrt{k/k_f}} \quad (17a)$$

with:

$$\text{Geo3} = \sqrt{\text{Nu}(H/W) \cdot (1+H/W)} \cdot \sqrt{\frac{H/W}{\delta_f/W}} + \frac{1}{2} \sqrt{\frac{\delta_f/W}{H/W}} \quad (17b)$$

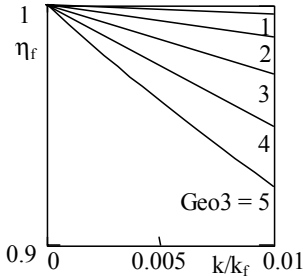


Fig. 3: Fin efficiency  $\eta_f(k/k_f, \text{Geo3})$  in relevant range (Equation 17)

Figure 3 shows, that a linear equation  $\eta_f = F(\text{Geo3})$  could approximate Equation 17a very well. But in the optimization Equation 17 is used, since with such a linear approximation the combined Equation 16 and 17 is still too complex to be solved analytically for  $H/W$  and  $\delta_f/W$ .

### OPTIMIZATION

The goal of the optimization is to find the optimum fin configuration expressed by  $H$ ,  $H/W$  and  $\delta_f/W$  for least pump power required. During the optimization, the optimum flow parameters such as velocity  $c$  and mass flow rate  $m$  are found implicitly.

The optima for the chosen design parameter are found by first analyzing Equations 15-17 analytically. These three equations are combined in order to contain only the chosen design parameters and the geometric parameters to be optimized for least pump power. Table 1a lists the design parameters that monotonically affect the pump power and the trend to minimize it, for a constant heat removal rate and base area. Thus, Table 1a tells the designer how to change the design point to obtain initially a lower fan/pump power before performing an optimization for fin geometry and flow parameters. All these parameters specify a nominal design point and are kept constant for the subsequent numerical optimization of the fin geometry.

Symbol	Optimum
$v$	Min
$\rho$	Max
$c_p$	Max
$k$	Max
$k/k_f$	Min
$Q$	Min
$\vartheta_1$	Max
$U$	Max
$A_b$	Max
$W_b/L_b$	Max

Table 1a: Optimum values for least pump power (initial values determining the design point)

The analytical analysis of Equations 15-17 gives no clear optimum for the following geometric design parameters:  $H$ ,  $H/W$ ,  $\delta_f/W$ . The separate evaluation of these equations suggests conflicting trends for minimal pump power, as summarized in Table 1b. From Equation 15a it is obvious that  $\vartheta_2$  and  $\text{Geo1}$  need to be minimized.  $\vartheta_2$  is minimum, if  $\vartheta_m$  is minimum (Figure 2); e.g.  $\text{Geo2}$  needs to be maximized (Equation 16a).  $\text{Geo2}$  is maximum if  $\eta_f$  is maximum, which is the case if  $\text{Geo3}$  is minimum as shown in Figure 3.

	Eq.	Opt.	H	H/W	$\delta_f/W$
Geo1	(15a)	Min	Max	Min	Min
Geo2	(16a)	Max	Min	Max	Min
Geo3	(17a)	Min	-	Min	2

Table 1b: Optimum geometric values for least pump power

The optimum values for  $H$ ,  $H/W$  and  $\delta_f/W$  can only be determined using a numerical optimization, specific to a set of values for the design parameters listed in Table 1a.

### Numerical Optimization

The optimum values of  $H$ ,  $H/W$ ,  $\delta_f/W$  are found numerically by Newton method.  $H$ ,  $H/W$  and  $\delta_f/W$  in Equations 15-17 are varied, while all design parameters in Table 1a are kept constant until the minimum pump power is found. In this optimization process, Equation 7 needs to be solved for  $\vartheta_2$  iteratively and all relevant flow parameters are found implicitly.

The fin height,  $H$ , was found to be the parameter of greatest importance, and will be discussed in the following paragraph.

The ratio of fin thickness to channel width  $\delta_f/W$ , exhibited similar trends, but of less importance. The aspect ratio of the channels  $H/W$ , came out to be maximized for minimum pump power within the investigated field. One explanation for this is the trend of Nusselt number and friction factor with aspect ratio. For numerical reason the maximum limit was set to  $H/W=100$ . In test optimizations with the maximum limit set to  $H/W=1000$ ,  $H/W$  also met the maximum limit. While channel width  $W$  and the ratio of fin thickness to channel width  $\delta_f/W$  then were approximately the same as with  $H/W=100$ , fin height  $H$  increased by factor 10 and fan/pump power decreased by same factor. Accordingly, for any other high aspect ratio  $H/W$  all results presented here may be adapted by scaling fin height and fan/pump power with the ratio of chosen upper limit  $H/W$  to 100.

Optima of  $H/W$  less than the upper limit could be found when  $H$  was constrained, as shown in the reference results below.

### Fin height effect

Since the fin height dominates the optimization, it will be discussed here in more detail. The heat transfer and the hydraulics introduce two competing effects that cause an optimum fin height, as illustrated in Figure 4. Combining Equations 1 and 2, fan power is determined by  $P=m(\zeta/2)c^2$  for  $\eta=1$ . On one hand, the heat transfer coefficient  $h$  decreases with increasing hydraulic diameter  $D_h$  (Equation 10), leading to increasing flow rate (Equation 6-8 and Figure 2). This is shown in Figure 4 by the increase in  $m$  as  $H$  approaches 2 cm. From the perspective of the hydraulics, the loss coefficient  $\zeta$  (which is part of the pressure drop Equation 2) increases with smaller hydraulic diameter. The product of  $m$  and  $\zeta$  gives a curve with a minimum. The effect is amplified by the curve of the through flow velocity  $c$  (Equation 5) shown in Figure 5, when calculating the pump power with  $P=m(\zeta/2)c^2$  (Figure 4). This basic trade-off between hydrodynamics and heat transfer is central in determining the optimal channel geometry. Fin efficiency  $\eta_f$ , overall efficiency  $\eta_o$  and total heat transfer area of a fin unit  $A_U$  appear to stay constant throughout the optimization since  $H/W$  is constant.

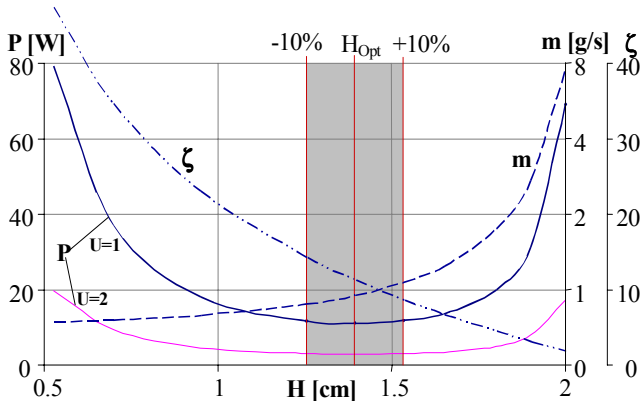


Fig. 4: Effect of fin height  $H$  on fan power  $P$ :  
air cooled, approach temperature  $32^\circ\text{C}$ ,  
base temperature  $84.5^\circ\text{C}$ , base area  $1\text{cm}^2$   
 $U=1$ ,  $Q=60\text{W}$ ,  $\eta=0.3$ ,  $H/W=100$ ,  $\delta_f/W=0.57$

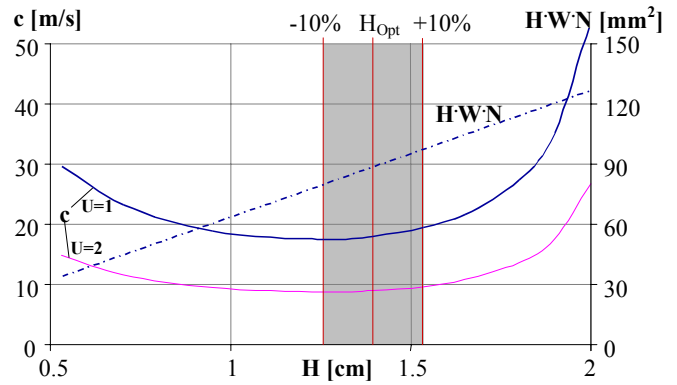


Fig. 5: Effect of fin height  $H$  on through flow velocity  $c$ :  
air cooled, approach temperature  $32^\circ\text{C}$ ,  
base temperature  $84.5^\circ\text{C}$ , base area  $1\text{cm}^2$   
 $U=1$ ,  $Q=60\text{W}$ ,  $\eta=0.3$ ,  $H/W=100$ ,  $\delta_f/W=0.57$

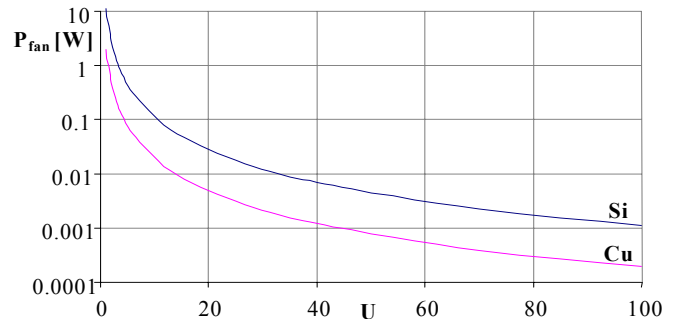


Fig. 6: Effect of Unit number  $U$  on fan power  $P$ :  
air cooled, approach temperature  $32^\circ\text{C}$ ,  
base temperature  $84.5^\circ\text{C}$ , base area  $1\text{cm}^2$   
 $Q=60\text{W}$ ,  $\eta=0.3$ ,  $H/W=100$ ,  $(\delta_f/W)_{\text{Si}}=0.57$ ,  $(\delta_f/W)_{\text{Cu}}=0.56$

### Unit number effect

For a given heat removal and base area, the unit number  $U$  changes only the through flow velocity as  $c \sim 1/U$  (Equation 5), while mass flow rate  $m$  and loss coefficient  $\zeta$  stay constant. Thus,  $U$  has a dramatic impact on the required fan/pump power as Figure 4 and 5 already have shown for one and two units and Figure 6 shows for 1 to 100 units. It can reduce fan/pump power by several orders favoring configurations with multiple fin units in parallel arrangement.

It should be mentioned here that this optimizing effect comes out so clear, because fully developed laminar flow is assumed and no entry length effect is considered, which implies that  $Nu$  and  $fRe$  are independent of velocity  $c$  and constant for constant aspect ratio  $H/W$ . However, the general trend will be similar if entry length effects are considered. Values may change, especially for extremely short units.

## RESULTS

In this section, the results of the above optimization are condensed in two design charts one for air cooled and one for water cooled heat sinks. Some general effects are outlined.

### Design charts

Figures 7 and 8 show the results of the numerical optimization for the minimized fan/pump power, in a five dimensional ( $Q$ ,

$k_f, \eta, U, W_b/L_b$  design space. Given the desired heat removal rate  $Q$  from a base area of  $1\text{cm}^2$  (abscise), and the conductivity ratio  $k/k_f$  (left ordinate) resulting from the chosen fin material, the optimum fin height  $H$  (dashed parameter curves), the optimum fin thickness/channel width ratio  $\delta_f/W$  (right ordinate) and the fan power needed (solid parameter curves) can be found. (The optimum channel aspect ratio is maximum  $H/W=100$ .) The actual power consumption of the fan/pump can be calculated knowing the fan/pump efficiency  $\eta$ , choosing the number of units  $U$  and the base aspect ratio  $W_b/L_b$ . The last two are expressed by the shape factor  $S$ :

$$S = \frac{W_b}{L_b} \Big|_{U=1} = \frac{W_b}{L_b} \cdot U^2 \quad (18)$$

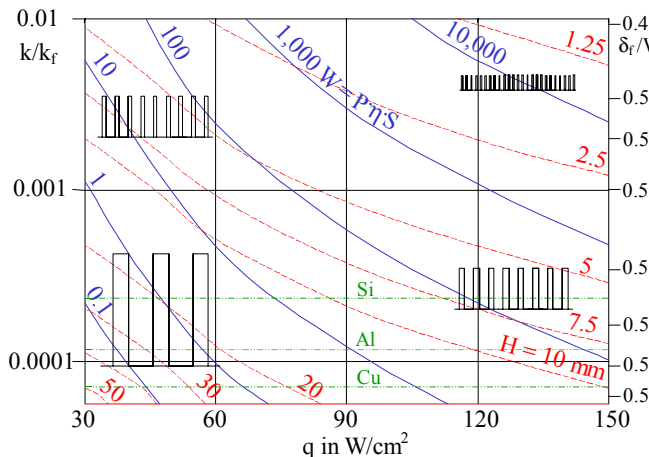


Fig. 7: Design chart for optimized heat sinks:  
air cooled, approach temperature  $32^\circ\text{C}$ ,  
base temperature  $84.5^\circ\text{C}$ , base area  $1\text{cm}^2$

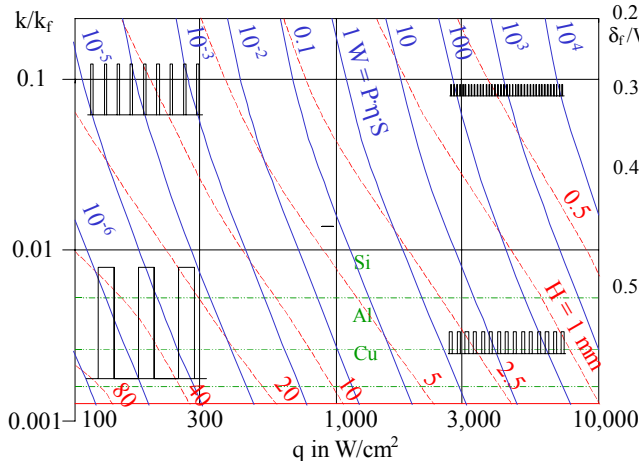


Fig. 8: Design chart for optimized heat sinks:  
water cooled, approach temperature  $20^\circ\text{C}$ ,  
base temperature  $84.5^\circ\text{C}$ , base area  $1\text{cm}^2$

### Effects

Changing the chosen unit number  $U$  in  $S$  shows how dramatically multi-unit configurations (Figure 1b-d) can

reduce fan/pump power compared to the configuration in Figure 1a with  $U=1$ .

The optimum fin height  $H$  decreases remarkably with heat rate  $Q$  and the conductivity ratio  $k/k_f$ .

The optimum ratio of fin thickness to channel width  $\delta_f/W$  depends only on the conductivity ratio fluid/fin  $k/k_f$ , and can hence be plotted directly on the right ordinate. In the design space for air, the optimum  $\delta_f/W$  changes only slightly around 0.5 with a maximum of 0.58 for  $k/k_f=0.00016$ , which lies between the conductivity ratio for silicon and aluminum. In the design space for water, the optimum  $\delta_f/W$  varies over a larger range of 0.2...0.55 and the maximum exists for a fin conductivity greater than that of cooper.

For the same heat rate  $Q$  and fin material using water instead of air as a coolant the optimum fin height  $H$  is approximately 8 times greater, where as optimum  $\delta_f/W$  is approximately 4% less.

The sketches in Figures 7 and 8 are not to scale concerning  $H$  and  $H/W=100$ , although  $H/W$  is constant for the sketches in each figure. These sketches shall give an idea how the heat sink design changes in each design space.

The effect of fin conductivity  $k_f$  on the power is shown in Figure 6. By using Cu instead of Si the fan/pump power can be reduced by one order of magnitude.

### Design Robustness

Figures 4 and 5 show a 10% margin for the optimum fin height. Within this margin, the change of fan power is very small. So, the design is considered to be robust within this range. A similar robustness can be observed for a change of inlet temperature difference  $\delta_i$  in a range of  $\pm 10\text{K}$ .

### Examples

Figure 7 indicates that with air as a coolant in a single-unit heat sink a heat flux of  $q=100\text{ W/cm}^2$  can be achieved with a fan power of 45W using a silicon heat sink, 16W for aluminum and 8W for cooper, assuming  $\eta=1$ . With a still easily practical two-unit arrangement, fan power reduces to 11W, 4W and 2W and with 100 fin units to 4.5mW, 1.7mW and 0.8mW.

Figure 8 indicates that with water as a coolant in a single-unit heat sink a heat flux of  $q=1\text{ kW/cm}^2$  can be achieved with a pump power of 25mW using silicon, 10mW using aluminum and 5mW using cooper, assuming again  $\eta=1$ . With a two-unit arrangement, pump power reduces to 6mW, 2.5mW and 1mW.  $q=10\text{ kW/cm}^2$  can be achieved with single fin unit and a pump power of 2.5kW using silicon, 1kW using aluminum and 0.5kW using cooper.

## ZIGZAG CONFIGURATION

### Zigzag analysis extension

The pressure drop in the inlet and outlet of the fin units (when multiple units are used) was not considered in the above analysis. It appears that a zigzag arrangement of the fin units allows a better velocity distribution in the unit inlet/outlet than a parallel arrangement of the units (Figures 1e and 9). Hence, the pressure loss will be less due to smaller velocity peaks.

The hydraulic diameter in the inlet and outlet is  $D_h=4H \cdot W_E/(2W_E+H)$ , where  $W_E$  is the inlet width for one unit. Since the hydraulic diameter and the aspect ratio  $H/(2W_E)$  in the inlet and outlet region are greater than for the channels between the fins the inlet/outlet velocity  $c_E$  can be higher by the velocity factor  $c_E=c \cdot cF$  for a comparable inlet/outlet pressure drop  $\Delta p_E \leq \Delta p$ . Thus, the necessary entrance width for each fin unit is  $W_E=N \cdot W/cF$  and with  $W_U^2=L_b^2+W_E^2$  the unit width  $W_U > L_b$  can be approximated to obtain a closed procedure by:

$$W_U = \frac{L_b \cdot (\delta_f + W)}{\sqrt{(\delta_f + W)^2 - (W/cF)^2}} \quad (19)$$

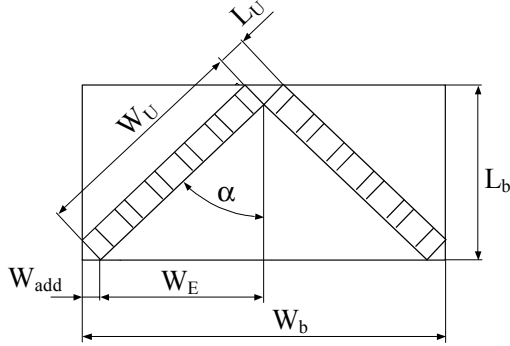


Fig. 9: Zigzag configuration

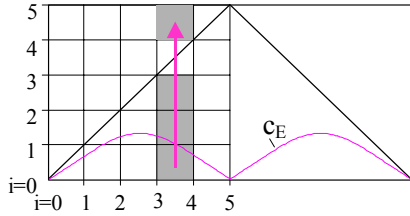


Fig. 10: Calculation inlet/outlet flow

For the flow calculation in the inlet and outlet region, it is assumed that the coolant flows through the zigzag arrangement in a parallel flow as Figure 10 shows. For one unit the flow is divided in  $I$  straight flow tubes of same width, with the aspect ratio  $H/\Delta W_E$ . The intersection with the fin unit divides the flow tubes in  $I$  length section  $\Delta L_b$ , which gives an array  $I \times I$ . The entry width for the hydraulic diameter  $D_{h,i}$  of each section  $i$  in flow direction is determined by  $2W_{E,i}=2W_{E,1}+(2W_{E,0}-2W_{E,1}) \cdot (I-i)/I$ , where  $W_{E,0}=W_E$  and for numerical reasons  $W_{E,1}=W$ . So  $fRe_i(H/2W_{E,i})$  is determined as for Equation 2. Equation 2 can be rewritten to  $(\zeta \cdot c)_i=fRe_i \Delta L_b \nu / D_{h,i}^2$ , where  $D_{h,i}=4H \cdot 2W_{E,i}/(2W_E+H)$ . The accuracy of incremental product  $(\zeta \cdot c)_i$  improves with  $(\zeta \cdot c)_i=(fRe_i+Re_{i-1})/2 \cdot \Delta L_b \nu / [(D_{h,i}+D_{h,i-1})/2]^2$ . The sum for the flow length  $L_b$  is calculated by:

$$(\zeta \cdot c)_{\text{sum},i} = \sum_{j=0}^{i-1} (\zeta \cdot c)_j + \sum_{j=0}^{I-1} (\zeta \cdot c)_j + \frac{(\zeta \cdot c)_i + (\zeta \cdot c)_{i-1}}{2} \quad (20)$$

where the first two sums are for the inlet and outlet region (gray in Figure 10) and the last term accounts for both triangle regions at the fin unit. Hence, Equation 2 can be written as:

$$c_i = \Delta p_{\text{guess}} \cdot (\zeta \cdot c)_{\text{sum},i} / 2 \rho \quad (21)$$

where  $c_i$  is the velocity in the stream tube  $i$  and  $\Delta p_{\text{guess}}$  is a first guess for the pressure drop in the inlet/outlet region.  $\Delta p_{\text{guess}}$  is calculated from an assumed fully developed laminar velocity profile, for which  $c_{\text{max}}=2c_m$  and  $c_m=c \cdot cF$ .

$$\Delta p_{\text{guess}} = 2 \cdot c \cdot cF \cdot \text{Min}_{j=0}^I ((\zeta \cdot c)_{\text{sum},j}) \cdot \frac{\rho}{2} \quad (22)$$

The minimum function selects the smallest  $(\zeta \cdot c)_{\text{sum}}$ , where the maximum velocity  $c_{\text{max}}$  exists. Assuming the same pressure drop occurs across each stream tube, now  $\Delta p_{\text{guess}}$  is corrected by

$$\Delta p_E = \Delta p_{\text{guess}} \cdot c \cdot cF \cdot \frac{I}{\sum_{j=1}^I c_j} \quad (23)$$

so that mass conservation is fulfilled. The overall pressure drop over the entire heat sink is then  $\Delta p_{\text{sum}}=\Delta p+\Delta p_E$  and  $\Delta p$  is calculated from Equation 2. In the analysis of Equations 2-14  $U$  is substituted by  $U=W_b/(W_{\text{add}}+W_E)$ , with  $W_{\text{add}}=L_U \cdot W_U/W_b$ . Analogous to the outlined hydraulic analysis, a convection analysis can be added for the inlet/outlet region. But for the optimized zigzag heat sinks, the contribution is typically around 1% and will be neglected, where as the pressure drop of the inlet/outlet region  $\Delta p_E$  adds around 50% to the overall pressure drop  $\Delta p_{\text{sum}}$ .

### Zigzag results

Figures 11a and 11b show the optimization results of the zigzag configuration. Figure 11a shows the parameters used previously, while Figure 11b shows the parameters unique to the zigzag configuration. The numerical optimization must now determine  $U$  and  $L_U$  in addition to  $H$ ,  $H/W$  and  $\delta_w/W$ . In the illustrated optimization,  $H/W$  reached again the upper limit which was set to 100. From Figures 11a it appears that the zigzag heat sink optimization results in more compact heat sinks with less fan/pump power consumption, although results in Figures 7 and 8 are obtained neglecting unit inlet/outlet pressure losses. For example, for a 90W heat removal rate from a 1cmx1cm base the optimized fin height and fan power for silicon and cooper heat sinks are  $H_{Si}=4.3(9.2)\text{mm}$ ,  $P_{Si}=4.3(88)\text{W}$ ,  $H_{Cu}=7.8(16.4)\text{mm}$ ,  $P_{Cu}=1.3(15)\text{W}$ , where the values in parentheses are from Figure 7 for a single unit heat sink with  $S=1$ .

The optimized zigzag heat sinks have typically a small unit angle  $\alpha=\arcsin(L_E/W_U)$  in the order of  $\alpha=2 \dots 5^\circ$ . With higher heat flux  $q$  the fan power, number of units  $U$  and velocity factor  $cF$  increase and the fin height  $H$ , fin unit length  $L_U$ , and the fin unit angle  $\alpha$  decrease. In the investigated field, the ratio  $\delta_f/W$  decreases negligible with  $\delta_f/W \sim 1/Q$ .

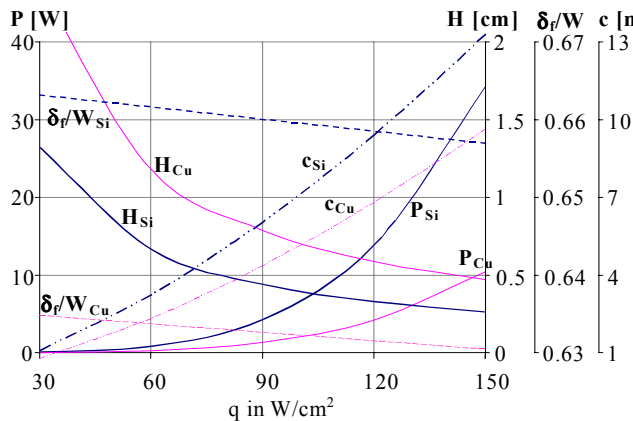


Fig. 11a: Optimized zigzag heat sinks: air cooled, approach temperature 32°C, base temperature 84.5°C, base area 1cm<sup>2</sup>, η=0.3

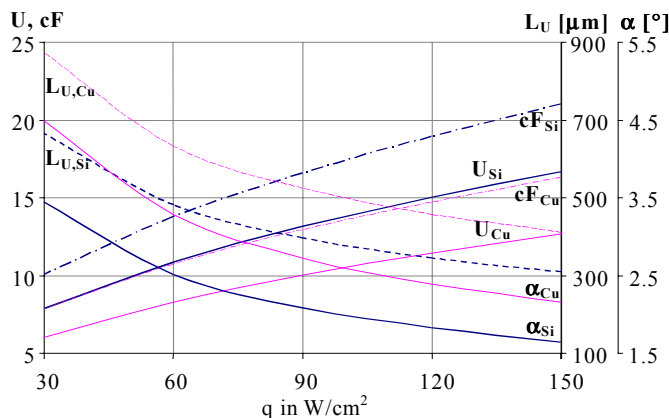


Fig. 11b: Optimized zigzag heat sinks: air cooled, approach temperature 32°C, base temperature 84.5°C, base area 1cm<sup>2</sup>, η=0.3

### REFERENCE RESULTS

Tuckerman and Pease [3] optimized a heat sink of 1cmx1cm made of silicon for water as a coolant. They found an optimum with  $\delta_f=W=57$ micron and  $H=365$ micron. With the reported  $11\text{cm}^3/\text{s}$  and a pressure drop of 206.8kPa(30psi), the pump power would be  $P=2.28\text{W}$  for  $\eta=1$ . In tests, the device reached up to  $Q=790\text{W}$ . For the reported  $\vartheta_1=71\text{K}$ , the same geometry and  $11\text{cm}^3/\text{s}$  the analyses after Equations 1-14 gives for  $k_f=148\text{W/m/K}$ :  $P=1.43\text{W}$ ,  $Q=1088\text{W}$ ,  $\Delta p=130.2\text{kPa}$ . Matching the reported pressure drop of 206.8kPa(30psi) the results are:  $P=3.6\text{W}$ ,  $Q=1170\text{W}$  and  $V=17.5\text{cm}^3/\text{s}$ . The optimization for  $Q=790\text{W}$  results in  $P=11.4\text{mW}$ ,  $\Delta p=2\text{kPa}$ ,  $H=6.38\text{mm}$ ,  $H/W=100$ ,  $\delta_f/W=0.50$ ,  $V=5.5\text{cm}^3/\text{s}$ . Copeland [4] performs an optimization for an air-cooled heat sink with fixed dimensions  $W_b=9\text{cm}$ ,  $L_b=6.5\text{cm}$ ,  $H=2.5\text{cm}$  (approximate size of near-future processor modules). He allows a maximum pressure drop of 40Pa and a maximum fan power of 0.215W and finds a minimal thermal resistance of 0.27C/W. Using the inlet temperature difference of 52.5K (as used in this work for air) this would give a heat rate of about 200W. The optimization for a single-unit heat sink after Equations 1-14 with  $\eta=1$  and  $k_f=240\text{W/m/K}$  assuming

aluminum results for  $P=0.215\text{W}$  in  $Q=306\text{W}$ ,  $\Delta p=34\text{Pa}$ ,  $c=3.4\text{m/s}$  (velocity in micro-channel),  $H/W=21.2$ ,  $\delta_f/W=0.212$ . This is equivalent to fin pitch 1.43mm and fin thickness of 0.25mm. It has to be mentioned that Copeland limited the fin pitch and thickness to 1.5mm and 0.3mm because those represent practical minima for corrugated and skived fin technology. However, Copeland found optima at fin pitch 2.3...2.4mm and fin thickness of 0.5mm. These dimensions give with Equations 1-14 and  $Q=200\text{W}$ :  $P=0.130\text{W}$ ,  $\Delta p=15\text{Pa}$ . For the same base configuration, the described zigzag optimization results with  $P=0.215\text{W}$  and  $\eta=1$  in  $Q=878\text{W}$ ,  $\Delta p=11.7\text{Pa}$ ,  $c=0.9\text{m/s}$  (in micro-channel),  $H/W=100$ ,  $\delta_f/W=0.586$ ,  $L_u=1.76\text{mm}$ ,  $\alpha=2.26^\circ$ .

### SUMMARY & CONCLUSIONS

The described optimization for least fan/pump power shows that for every heat removal, base area and aspect ratio there is an optimum fin height and ratio fin thickness/channel width. The channel aspect ratio always tends to be maximized, when the fin height is not fixed during the optimization. With increased heat removal, the optimum fin height decreases, while fan/pump power increases. The optimum ratio of fin thickness to channel width using water is about 0.5 and using air 0.57. Design charts for both coolants show the trends of optimized parameters such as fan/pump power, fin height and the ratio fin thickness to channel width. Multi fin-units in parallel flow arrangement can reduce fan/pump power by several orders of magnitude. With the optimizing tool, configurations for heat removal of 100W/cm<sup>2</sup> with air and 10kW with water and a pump power expense of less than 1% could easily be found. Optimized zigzag arrangements are preferable to parallel arrangement of fin units. They are smaller and require less pump power for the same heat removal.

### REFERENCES

- [1] I. Mudawar: "Assessment of high-heat-flux thermal management schemes", IEEE Transactions on Components and Packaging, Vol. 24/2, 2001, pp. 122 -141.
- [2] International roadchart of semiconductors, <http://www.itrs.net/public/>.
- [3] D. B. Tuckerman and R. F. W. Pease, "High-Performance Heat Sinking for VLSI", IEEE Electron Device Letters, Vol. EDL-2, No. 5, May 1981, pp. 126-129.
- [4] D. Copeland "Optimization of parallel plate heatsinks for forced convection", Semiconductor Thermal Measurement and Management Symposium, 21-23 March 2000. (16th Annual IEEE), pp. 266 -272.
- [5] C. B. Sobhan and S. V. Garimella, "A comparative analysis of studies on heat transfer and fluid flow in microchannels", Microscale Thermophysical Engineering, Vol. 5, 2001, pp. 293-311.
- [6] Y. A. Cengel. *Introduction to thermodynamics and heat transfer*, McGraw-Hill, New York, 1997.
- [7] F.P. Incropera *Introduction to heat transfer*, Wiley, New York, 1996.
- [8] D. R. Harper and Brown W. B. "Mathematical equations for heat conduction in the fins of air cooled engines", NACA Report No. 158, 1922.
- [9] P. J. Schneider. *Conduction heat transfer*, Addison-Wesley, Reading MA, 1955.